https://science.utm.my/procscimath
Volume 21 (2024) 169-179

Mixed Convection Boundary Layer Flow of Viscoelastic Hybrid Nanofluid Past Over a Sphere with Constant Heat Flux

Mohamad Solahudin Ibrahim, Wan Rukaida Wan Abdullah*
Department of Mathematical Sciences, Faculty of Science, Universiti Teknologi Malaysia
*Corresponding author: wrukaida@utm.my

Abstract
The study focuses on the mixed convection boundary layer flow of a viscoelastic hybrid nanofluid passing over a sphere with a constant heat flux. This study examines copper (Cu) and aluminium oxide ($\mathrm{Al_2O_3}$) nanoparticles using water ($\mathrm{H_2O}$) as the base fluid. Using the Tiwari-Das model, the governing boundary layer equations are first changed into non-dimensional forms by using specific dimensionless variables. Furthermore, the MATLAB BVP4C solver is utilised in this work to create a numerical computer simulation to evaluate the flow behaviour as impacted by viscoelastic factors and the heat properties of the hybrid nanofluid model. The findings are visually shown to demonstrate the effects of the viscoelastic parameter, *K*, mixed convection parameter, λ, heat generation effect, γ, nanoparticle volume fraction parameter, $\emptyset$, and Prandtl number, Pr on the velocity and temperature profiles. Graphs are used to analyse the relationship between various metrics, such as velocity and temperature profiles, as well as skin friction and heat transfer. Increasing the heat generation effect, γ, leads to higher velocity and temperature profiles, as previously described. Increasing γ values often results in larger velocity and temperature distributions. As γ grows, the velocity and thickness of the thermal boundary layer increase. Next, both the velocity and temperature profiles decrease as Pr, rises. Finally, increasing the value of the $\emptyset$ and λ leads to an increase in both nanofluid flow and temperature distribution.
Keywords: Mixed convection; boundary layer flow; viscoelastic; hybrid nanofluid; sphere; constant heat flux; BVP4C solver

Introduction

Nanofluids, comprising nanoparticles in a base fluid, show improved heat transfer and thermophysical properties [1,2]. Hybrid nanofluids, combining different nanoparticles, aim to optimize their benefits. Despite lower conductivity, alumina is favoured for stability. Combining metallic (e.g., copper, silver, gold) with non-metallic (e.g., carbon nanotubes, graphene) nanoparticles creates hybrids with specialized features, enhancing fluid performance.

Hybrid nanofluids have a range of applications, notably in enhancing heat transfer efficiency. They are used in heat exchangers, cooling systems, and electronic devices to improve thermal performance. The efficiency of a $\mathrm{Cu} - \mathrm{Fe_3O_4}/\mathrm{H_2O}$ hybrid nanofluid in a hydromagnetic flow inspired by biological systems [3]. These fluids are especially useful in electronic cooling systems, where they help dissipate heat from components, preventing overheating and increasing the reliability of electronic equipment. By combining the strengths of various nanoparticles, hybrid nanofluids offer tailored solutions for improving thermal management in various fields.

Viscoelasticity combines viscosity and elasticity, describing time-dependent material deformation under stress. Initial studies focused on isotropic materials' stress-deformation relationships [4], later examining small deformations on large stretches [5]. Viscoelastic fluids don't move far or quickly from their shape [6], affecting flow past circular cylinders [7]. These fluids are crucial in chemical, nuclear, geophysical, material processing, and bioengineering fields [8].

A viscoelastic hybrid nanofluid combines viscoelastic properties with enhanced thermal conductivity, improving heat transfer and flow management. Ideal for advanced thermal management and electronic cooling, these fluids dissipate heat efficiently while handling mechanical stress and

vibrations. Their unique properties make them suitable for applications needing both effective heat transmission and the ability to withstand dynamic mechanical forces.

Mixed convection combines natural and forced convection in a fluid [9]. It occurs when fluid flows along a solid surface, with heat transfer influenced by external forces and temperature-driven buoyancy. Forced convection is driven by fans or pumps, enhancing fluid velocity near the surface, while natural convection arises from buoyancy forces due to temperature differences. This effect is common in heat exchangers, electronic cooling, and environmental processes.

In mixed convection boundary layer flow, fluid behaviour near a solid surface is influenced by both forced and natural convection. Forced convection, driven by fans or pumps, increases fluid velocity near the surface. Natural convection, caused by buoyancy forces from temperature changes, makes heated fluid rise and cooled fluid sink, aiding vertical fluid flow and heat transfer. Together, these forces enhance heat transfer efficiency in various engineering applications.

Literature Review

Constant mixed convection flow over a vertical surface in a porous medium was examined using hybrid nanoparticles [10]. Alumina (Al_2O_3) and copper (Cu) nanoparticles suspended in water formed an $Al_2O_3 - Cu$/water hybrid nanofluid. Similarity equations were derived from governing equations using similarity variables and solved with MATLAB's bvp4c solver. Mixed convective heat transfer in a square enclosure with two layers and a spinning circular cylinder in the center was numerically investigated [11]. The upper layer comprised Al_2O_3-water nanofluid, while the bottom layer was a porous medium. Horizontal walls were insulated, and temperature differences were maintained across the vertical walls. The dimensionless governing equations were solved using the Galerkin finite element method.

Two-dimensional mixed convection radiative nanofluid flow over a wavy inclined surface in a non-Darcy permeable medium was investigated [12]. The wavy surface was transformed into a flat one for analysis, considering heat source, thermal radiation, and chemical reaction rate. Using a similarity framework, nonlinear partial differential equations were converted into dimensionless ordinary differential equations (ODEs). These ODEs were solved using MATLAB's parametric continuation method (PCM). Results affirmed reliability and effectiveness compared to prior studies.

Mixed convection in a porous trapezoidal cavity filled with a $Cu - Al_2O_3$/water hybrid nanofluid was studied [13]. The governing equations were solved numerically using a finite difference method in dimensionless form. The study investigated streamlines and isotherms, analyzing the impact of factors like Reynolds number, Darcy number, and nanoparticle volume percentage on the numerical results. Nanofluid research is growing in industrial and engineering fields. Mixed convection flow around a symmetric cylinder in a viscoelastic nanofluid with viscous dissipation was analyzed [14].

Nanofluid flow is advantageous for cooling electronic equipment, leading to significant energy savings. The horizontal analysis of radiation effects on mixed convection of Walters'-B nanofluid flow in a circular cylinder with constant heat flux (CHF) and convective boundary conditions (CBC) were focused [15]. They used sodium carboxymethyl cellulose (CMC-water) nanofluid containing copper nanoparticles. The Keller-box numerical method was employed to simplify the partial differential equations. Due to its practical applications, heat transfer involving non-Newtonian fluids in porous areas has garnered significant attention.

The mixed convection flow of a viscoelastic hybrid nanofluid past a spinning disc was examined [16]. Alumina (Al_2O_3) and silver (Ag) nanoparticles were dispersed in carboxymethyl cellulose (CMC)-water. The study considered a viscoelastic fluid model and magnetic field effects. Nonlinear differential equations were solved using the Galerkin finite element method. The heat and mass transfer properties of magneto-hydrodynamic mixed convective viscoelastic hybrid nanofluid flow on an extending spinning disc were examined [17]. Entropy generation, thermal radiation, convective conditions, and slips were studied. The hybrid nanofluid included aluminium nitride and alumina nanoparticles in carboxymethyl cellulose, with concentrations from 0.0% to 0.4%. Equations were transformed and solved using the Galerkin method.

Mathematical Model

Mathematical Formulation of Viscoelastic Hybrid Nanofluid Past Over a Sphere

This study examines fluid flow across a sphere with radius a, submerged in a viscoelastic hybrid nanofluid. The velocity outside the boundary is $\bar{u}_e(\bar{x})$, with u and v representing fluid velocity components along x and y. Table 1 shows the thermophysical properties of the hybrid nanofluid, including dynamic viscosity, heat capacity, density, thermal conductivity, and thermal expansion. The terms $f, nf, hnf,$ and np denote base fluid, nanofluid, hybrid nanofluid, and nanoparticles ($np1$ and $np2$ for the first and second nanoparticles). The symbols $\emptyset_1$ and $\emptyset_2$ represent the solid volume fractions of the nanoparticles.

Table 1: Hybrid nanofluid thermophysical properties, [24, 25]

Properties	**Hybrid Nanofluid**
Density	$\rho_{hnf} = (1-\emptyset_{np2})\left[(1-\emptyset_{np1})\rho_{bf} + \emptyset_{np1}\rho_{np1}\right] + \emptyset_{np2}\rho_{np2},$
Dynamic viscosity	$\mu_{hnf} = \frac{\mu_{bf}}{(1-\emptyset_{np1})^{2.5}(1-\emptyset_{np2})^{2.5}},$
Volumetric heat capacity	$(\rho C_p)_{hnf} = (1-\emptyset_{np2})\left[(1-\emptyset_{np1})(\rho C_p)_{bf} + \emptyset_{np1}(\rho C_p)_{np1}\right] + \emptyset_{np2}(\rho C_p)_{np2},$
Thermal conductivity	$\frac{k_{hnf}}{k_{bf}} = \frac{k_{np2}+(n-1)k_{bf}-(n-1)\emptyset_{np2}(k_{bf}-k_{np2})}{k_{np2}+(n-1)k_{bf}+\emptyset_{np2}(k_{bf}-k_{np2})}$, where $\frac{k_{nf}}{k_f} = \frac{(n-1)k_{bf}+k_{np1}-(n-1)\emptyset_{np1}(k_{bf}-k_{np1})}{(n-1)k_{bf}+k_{np1}+\emptyset_{np1}(k_{bf}-k_{np1})},$
Thermal expansion	$(\rho\beta)_{hnf} = (1-\emptyset_{np2})\left[(1-\emptyset_{np1})(\rho\beta)_{bf} + \emptyset_{np1}(\rho\beta)_{np1}\right] + \emptyset_{np2}(\rho\beta)_{np2}$

Figure 1 shows the physical model and coordinate system [20]. T_w define as the sphere's surface temperature and T_∞ define as the hybrid nanofluid's ambient temperature [21]. They state that $T_w < T_\infty$ indicates a cooling sphere (opposing flow), while $T_w > T_\infty$ indicates a heating sphere (assisting flow). The velocity of the continuous free stream was assumed as $\frac{1}{2}U_\infty$ [22].

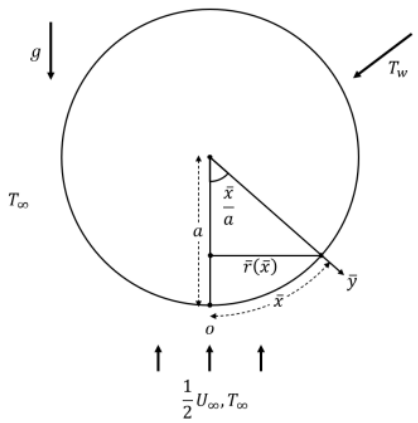

Figure 1 Coordinates system and flow model, [20]

The three equations were produced [20]:
Continuity Equation:

$$\frac{\partial}{\partial \bar{x}}(\bar{r}\bar{u}) + \frac{\partial}{\partial \bar{y}}(\bar{r}\bar{v}) = 0, \tag{1}$$

Momentum Equation:

$$\rho_{hnf}\left(\bar{u}\frac{\partial \bar{u}}{\partial \bar{x}} + \bar{v}\frac{\partial \bar{u}}{\partial \bar{y}}\right) = \rho_{hnf}\left(\bar{u}_e\frac{\partial \bar{u}_e}{\partial \bar{x}}\right) + \mu_{hnf}\left(\frac{\partial^2 \bar{u}}{\partial \bar{y}^2}\right) + k_0\left[\frac{\partial}{\partial \bar{x}}\left(\bar{u}\frac{\partial^2 \bar{u}}{\partial \bar{y}^2}\right)\right] + \bar{v}\frac{\partial^3 \bar{u}}{\partial \bar{y}^3} + \frac{\partial \bar{u}}{\partial \bar{y}}\frac{\partial^2 \bar{v}}{\partial \bar{y}^2} + g(\rho\beta)_{hnf}(T - T_\infty)\sin\left(\frac{\bar{x}}{a}\right), \tag{2}$$

Energy Equation:

$$\bar{u}\frac{\partial T}{\partial \bar{x}} + \bar{v}\frac{\partial T}{\partial \bar{y}} = \alpha_{hnf}\frac{\partial^2 T}{\partial \bar{y}^2}, \tag{3}$$

where:
α_{hnf} = Thermal diffusivity of hybrid nanofluid
ρ_{hnf} = Density of hybrid nanofluid
μ_{hnf} = Dynamic density of hybrid nanofluid
$\left(\rho C_p\right)_{hnf}$ = Volumetric heat capacity of hybrid nanofluid
$(\rho\beta)_{hnf}$ = Thermal expansion of hybrid nanofluid
$\frac{k_{hnf}}{k_{bf}}$ = Thermal conductivity of hybrid nanofluid
$\frac{k_{nf}}{k_f}$ = Thermal conductivity of nanofluid

Subject to boundary conditions:

$$\bar{u} = 0, \quad \bar{v} = 0, \quad T = -\frac{q_w}{k_{nf}}, \quad \text{on} \quad \bar{y} = 0, \quad \bar{x} \geq 0 \tag{4}$$

$$\bar{u} = \bar{u}_e(\bar{x}), \quad \frac{\partial \bar{u}}{\partial \bar{y}} = 0, \quad T = T_\infty, \quad \text{as} \quad \bar{y} \to \infty, \quad \bar{x} \geq 0,$$

Here $\bar{x}$ and $\bar{y}$ are Cartesian coordinates on the sphere's surface, with $\bar{y}$ normal to the surface. $\bar{u}$ and $\bar{v}$ are velocity components, g is gravity, n is flow direction, T is fluid temperature, $k_0 > 0$ is the viscoelastic constant (Walter's Liquid-B model), v is kinematic viscosity, and $\emptyset$ is nanoparticle volume fraction. Nanoparticles Cu and $\mathrm{Al_2O_3}$ are $np1$ and $np2$. The equations include thermal expansion coefficient (β), heat capacitance (C_p), thermal conductivities (k), density (ρ), dynamic viscosities (μ), and thermal diffusivities (α). $\bar{u}_e(\bar{x})$ is the local free stream velocity, and $\bar{r}(\bar{x})$ is the radial distance from the symmetry axis to the sphere's surface.

$$\bar{u}_e(\bar{x}) = \frac{3}{2}U_\infty \sin\left(\frac{\bar{x}}{a}\right) \text{ and } \bar{r}(\bar{x}) = \alpha \sin\left(\frac{\bar{x}}{a}\right).$$

The thermal conductivity data in table 2 matches experimental results well [18]. The high agreement supports using their thermophysical characteristics in this study. This research involves two nanoparticles, Alumina ($\mathrm{Al_2O_3}$) and Copper (Cu), with water ($\mathrm{H_2O}$) as the base fluid. Table 2 presents the thermophysical characteristics of various nanoparticles and base fluids.

Table 2: Thermophysical characteristic of Aluminium Oxide ($\mathrm{Al_2O_3}$), Copper (Cu) and water ($\mathrm{H_2O}$), [24,25,29]

Properties	$\mathbf{Al_2O_3}$	$\mathbf{Cu}$	$\mathbf{H_2O}$
$\boldsymbol{\rho(kg/m^3)}$	3970	8933	997.1
$\boldsymbol{C_p(J/kgK)}$	765	385	4179
$\boldsymbol{k(W/mK)}$	40	400	0.613
$\boldsymbol{\beta_T(K^{-1})}$	0.67×10^{-5}	1.67×10^{-5}	21×10^{-5}

Dimensionless Governing Equations

The dimensionless governing equations can be obtained as below,

Continuity Equation:

$$\frac{\partial}{\partial x}(ru)+\frac{\partial}{\partial y}(rv)=0, \tag{5}$$

Momentum Equation:

$$\begin{aligned}\left[\left(1-\emptyset_{np2}\right)\left(\left(1-\emptyset_{np1}\right)+\emptyset_{np1}\frac{\rho_{np1}}{\rho_{bf}}\right)+\emptyset_{np2}\frac{\rho_{np2}}{\rho_{bf}}\right]\left(u\,\frac{\partial u}{\partial x}+v\,\frac{\partial u}{\partial y}\right)\\ =\left[\left(1-\emptyset_{np2}\right)\left(\left(1-\emptyset_{np1}\right)+\emptyset_{np1}\frac{\rho_{np1}}{\rho_{bf}}\right)+\emptyset_{np2}\frac{\rho_{np2}}{\rho_{bf}}\right]\left(u_e\,\frac{\partial u_e}{\partial x}\right)\\ +\frac{1}{\left(1-\emptyset_{np1}\right)^{2.5}\left(1-\emptyset_{np2}\right)^{2.5}}\left(\frac{\partial^2 u}{\partial y^2}\right)+K\left(\frac{\partial u}{\partial x}\,\frac{\partial^2 u}{\partial y^2}+v\,\frac{\partial^3 u}{\partial y^3}+\frac{\partial u}{\partial y}\,\frac{\partial^2 v}{\partial y^2}\right)\\ +\lambda\theta\sin(x)\left[\left(1-\emptyset_{np2}\right)\left(1-\emptyset_{np1}\right)+\emptyset_{np1}\frac{(\rho\beta)_{np1}}{(\rho\beta)_{bf}}+\emptyset_{np2}\frac{(\rho\beta)_{np2}}{(\rho\beta)_{bf}}\right],\end{aligned} \tag{6}$$

Energy Equation:

$$\begin{aligned}\left[\left(1-\emptyset_{np2}\right)\left[\left(1-\emptyset_{np1}\right)+\emptyset_{np1}\frac{(\rho C_p)_{np1}}{(\rho C_p)_{bf}}\right]+\emptyset_{np2}\frac{(\rho C_p)_{np2}}{(\rho C_p)_{bf}}\right]\left[u\frac{\partial\theta}{\partial x}+v\frac{\partial\theta}{\partial y}\right]\\ =\frac{1}{Pr}\left[\frac{k_{np2}+(n-1)k_{bf}-(n-1)\emptyset_{np2}\left(k_{bf}-k_{np2}\right)}{k_{np2}+(n-1)k_{bf}+\emptyset_{np2}\left(k_{bf}-k_{np2}\right)}\right]\frac{\partial^2\theta}{\partial y^2},\end{aligned} \tag{7}$$

by substituting the dimensionless variables [30,31] into equations (1), (2) and (3). The dimensionless variables are:

$$\begin{aligned}x=\frac{\bar{x}}{a},\qquad y=Re^{\frac{1}{2}}\left(\frac{\bar{y}}{a}\right),\qquad u=\frac{\bar{u}}{U_\infty},\qquad v=Re^{\frac{1}{2}}\left(\frac{\bar{v}}{U_\infty}\right),\\ r(x)=\frac{\bar{r}(\bar{x})}{a},\qquad u_e(x)=\frac{\bar{u}_e(x)}{U_\infty},\qquad \theta=\frac{(T-T_\infty)}{(T_w-T_\infty)},\end{aligned} \tag{8}$$

where $Re=\frac{U_\infty a}{v}$ is the Reynolds Number.

The boundary conditions change into:

$$\begin{aligned}u=0,\quad v=0,\quad \theta'=-1,\quad \text{on}\quad \text{y}=0,\quad x\geq 0,\\ u=u_e(x)=\frac{3}{2}\sin x,\quad \frac{\partial u}{\partial y}=0,\quad \theta=0,\quad \text{as}\quad y\to\infty,\quad x\geq 0,\end{aligned} \tag{9}$$

where:

$K=\frac{k_0 U_\infty}{av\rho_{bf}}$ is the dimensionless viscoelastic parameter,

$Pr=\frac{v}{a_{bf}}$ is the Prandtl number,

$\lambda=\frac{Gr}{Re^2}=\frac{g\beta_{bf}(T_w-T_\infty)a}{{U_\infty}^2}$ is the constant mixed convection parameter.

$\lambda<0$ correspond to a cooling sphere (opposing flow),

$\lambda>0$ corresponds to a heating sphere (assisting flow),

Forced convection flow when $\lambda=0$.

Transformation of the Dimensionless Governing Equations

To solve the equations (5), (6) and (7) by using the boundary conditions from equation (9), the following variables are being assumed as:

$$\psi=xr(x)f(x,y),\qquad \theta=\theta(x,y). \tag{10}$$

Then, factorise U_∞ and becomes,

$$u = \frac{1}{r}\frac{\partial \psi}{\partial y}, \qquad v = -\frac{1}{r}\frac{\partial \psi}{\partial x}. \tag{11}$$

Substitute equations (5), (6), (7), and (9) with the equation (11). Then consider $u_e(x) = \frac{\bar{u}_e(\bar{x})}{U_\infty} = \frac{3}{2}\sin x$ and $r(x) = \sin x$. The equations become:

Continuity Equation:

$$\frac{\partial^2 \psi}{\partial x \partial y} - \frac{\partial^2 \psi}{\partial x \partial y} = 0, \tag{12}$$

Momentum Equation:

$$\begin{aligned} C_1\left[\frac{-\cos x}{\sin x}\left(\frac{\partial f}{\partial y}\right)^2 + x\left(\frac{\partial f}{\partial y}\frac{\partial^2 f}{\partial x \partial y} - \frac{\partial f}{\partial x}\frac{\partial^2 f}{\partial y^2}\right) + \left(\frac{x\cos x}{\sin x} + 1\right)\left(\left(\frac{\partial f}{\partial y}\right)^2 - \frac{\partial^2 f}{\partial y^2} f\right)\right] \\ = C_1\left(\frac{9}{4}\frac{\sin x \cos x}{x}\right) + C_2\left(\frac{\partial^3 f}{\partial y^3}\right) \\ + K\left[x\frac{\partial^3 f}{\partial y^3}\frac{\partial^2 f}{\partial x \partial y} + 2\left(\frac{x\cos x}{\sin x} + 1\right)\left(\frac{\partial f}{\partial y}\frac{\partial^3 f}{\partial y^3}\right) + \left(x\frac{\partial^4 f}{\partial x \partial y^3}\frac{\partial f}{\partial y}\right)\right. \\ - 2\left(\frac{x\cos x}{\sin x}\right)\left(\frac{\partial f}{\partial y}\frac{\partial^3 f}{\partial y^3}\right) - \left(x\frac{\partial f}{\partial x}\frac{\partial^4 f}{\partial y^4}\right) - \left(\frac{x\cos x}{\sin x} + 1\right)\frac{\partial^4 f}{\partial y^4} f - \left(x\frac{\partial^2 f}{\partial y^2}\frac{\partial^3 f}{\partial x \partial y^2}\right) \\ \left. - \left(\frac{x\cos x}{\sin x} + 1\right)\left(\frac{\partial^2 f}{\partial y^2}\frac{\partial^2 f}{\partial y^2}\right)\right] + C_3 \lambda \theta \frac{\sin(x)}{x}, \end{aligned} \tag{13}$$

Energy Equation:

$$C_4\left[\left(x\frac{\partial f}{\partial y}\frac{\partial \theta}{\partial x}\right) - \left(\left(x\frac{\partial f}{\partial y}\right) + \left(1 + x\frac{\cos x}{\sin x}\right) f\right)\frac{\partial \theta}{\partial y}\right] = C_5\frac{1}{\mathrm{Pr}}\frac{\partial^2 \theta}{\partial y^2}, \tag{14}$$

The boundary conditions change as follow,

$$\begin{aligned} &f = 0, \quad \frac{\partial f}{\partial y} = 0, \quad \theta' = -1, \quad \text{on} \quad \mathrm{y} = 0, \quad x \geq 0, \\ &\frac{\partial f}{\partial y} \to \frac{3}{2}\frac{\sin x}{x}, \quad \frac{\partial^2 f}{\partial y^2} = 0, \quad \theta \to 0, \quad \text{as} \quad y \to \infty, \quad x \geq 0, \end{aligned} \tag{15}$$

where at the lower stagnation point of the sphere $x \approx 0$, the equations (13) and (14) become ordinary differential equations as below,

Momentum Equation:

$$C_1\left(2ff'' - f'^2 + \frac{9}{4}\right) + C_2 f''' + 2K\left(f'f''' - ff'''' - f''^2\right) + C_3\lambda\theta = 0, \tag{16}$$

Energy Equation:

$$2C_4 f\theta' + C_5\frac{1}{\mathrm{Pr}}\theta'' = 0, \tag{17}$$

where:

$$C_1 = \left(1 - \emptyset_{np2}\right)\left(\left(1 - \emptyset_{np1}\right) + \emptyset_{np1}\frac{\rho_{np1}}{\rho_{bf}}\right) + \emptyset_{np2}\frac{\rho_{np2}}{\rho_{bf}},$$

$$C_2 = \frac{1}{\left(1-\emptyset_{np1}\right)^{2.5}\left(1-\emptyset_{np2}\right)^{2.5}},$$

$$C_3 = \left(1 - \emptyset_{np2}\right)\left(1 - \emptyset_{np1}\right) + \emptyset_{np1}\frac{(\rho\beta)_{np1}}{(\rho\beta)_{bf}} + \emptyset_{np2}\frac{(\rho\beta)_{np2}}{(\rho\beta)_{bf}},$$

$$C_4 = \left(1 - \emptyset_{np2}\right)\left[\left(1 - \emptyset_{np1}\right) + \emptyset_{np1}\frac{(\rho C_p)_{np1}}{(\rho C_p)_{bf}}\right] + \emptyset_{np2}\frac{(\rho C_p)_{np2}}{(\rho C_p)_{bf}},$$

$$C_5 = \frac{k_{np2} + (n-1)k_{bf} - (n-1)\emptyset_{np2}\left(k_{bf} - k_{np2}\right)}{k_{np2} + (n-1)k_{bf} + \emptyset_{np2}\left(k_{bf} - k_{np2}\right)}.$$

Then, the boundary conditions become,

$$\begin{aligned} &f = 0, \quad \frac{\partial f}{\partial y} = 0, \quad \theta' = -1, \quad \text{on} \quad \mathrm{y} = 0, \quad x \geq 0, \\ &\frac{\partial f}{\partial y} \to \frac{3}{2}, \quad \frac{\partial^2 f}{\partial y^2} = 0, \quad \theta \to 0, \quad \text{as} \quad y \to \infty, \quad x \geq 0. \end{aligned} \tag{18}$$

The equations (16), (17) and (18) are used to investigate the behaviour of mixed convection boundary later flow of viscoelastic in hybrid nanofluid.

Numerical Methods

The BVP4C solver in MATLAB addresses boundary value problems (BVPs) in science and engineering. It was used for steady two-dimensional hydromagnetic convective flow in a porous medium [23], mixed convection flow over a vertical surface with hybrid nanoparticles [10], thermal radiation and Newtonian heating effects [24], and hybrid nanofluid boundary layer flow [25]. The solver integrates first-order problem equations with boundary conditions using sol = bvp4c(odefun, bcfun, solinit) and initial guesses with bvpinit [18].

The following is expressed as a first-order equation:

$$y_1 = f, \quad y_2 = f', \quad y_3 = f'', \quad y_4 = f''', \quad {y_4}' = f'''', \tag{19}$$
$$y_5 = \theta, \quad y_6 = \theta', \quad {y_6}' = \theta''.$$

From the equations (16) and (17), the equations can be transformed into the first order equation as below:

Momentum Equation:

$${y_4}' = \frac{1}{y_1}\left[{y_2}y_4 - {y_3}^2 + \frac{1}{2K}\left(C_1\left(2y_1y_3 - {y_2}^2 + \frac{9}{4}\right) + C_2y_4 + C_3\lambda y_5\right)\right], \tag{20}$$

Energy Equation:

$${y_6}' = -\frac{Pr}{C_5}(2C_4y_1y_6), \tag{21}$$

The boundary conditions become:

$$y_1(0) = 0, \quad y_2(0) = 0, \quad y_6(0) = -1, \tag{22}$$
$$y_2(\infty) = \frac{3}{2}, \quad y_3(\infty) = 0, \quad y_5(\infty) = 0.$$

MATLAB algorithms utilized first-order differential equations (20) and (21) with boundary conditions (equation (22)). Adjustments were made for varying parameters (*K*, Pr, λ, and ∅), generating velocity and temperature profile graphs. The velocity and temperature profiles of a viscoelastic hybrid nanofluid were solved using copper (Cu) and aluminium oxide (Al_2O_3). The goal is to identify $Cu - Al_2O_3$, is better for the behaviour of fluid flow past a sphere for future usage.

Results and Discussion

Equations (20) and (21) with boundary conditions in Equation (22) are used to solve viscoelastic hybrid nanofluid past over a sphere using hybrid nanofluid algorithms in equation (19) at lower stagnation point $x \approx 0$. This topic considers parameter values for all thermophysical parameters, such as density (ρ), heat capacitance (Cp), thermal conductivity (k) and dynamic viscosity (μ) for nanoparticle Cu ($np1$) and Al_2O_3 ($np2$).

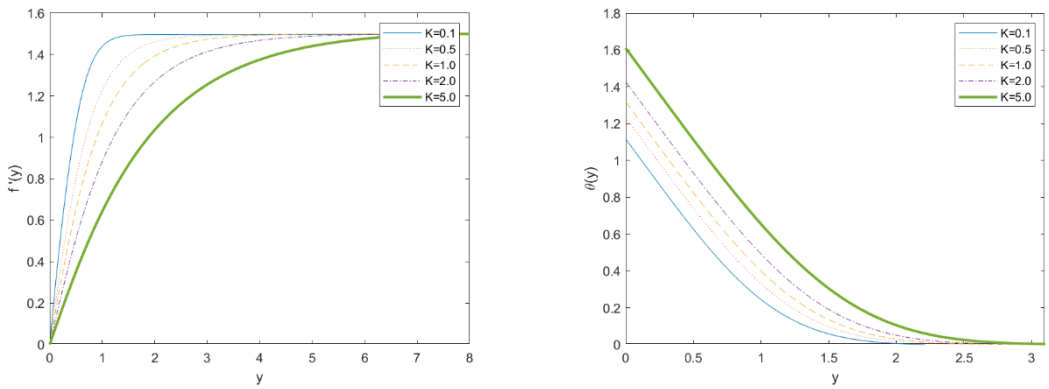

Figure 2 Velocity and Temperature profiles for different value of *K*.

Figure 2 display velocity and temperature profiles of a hybrid nanofluid at the lower stagnation point ($x \approx 0$) for various *K* values ($\mathrm{Pr} = 1, \emptyset = 0.1, \lambda = 1$). Increasing *K* leads to lower velocity and higher temperature profiles. As *K* increases, the velocity and temperature profiles become less steep. Boundary layer thickness increases with *K*, suggesting enhanced heat transfer in hybrid nanofluids by promoting quicker temperature reduction and velocity increase compared to nanofluids.

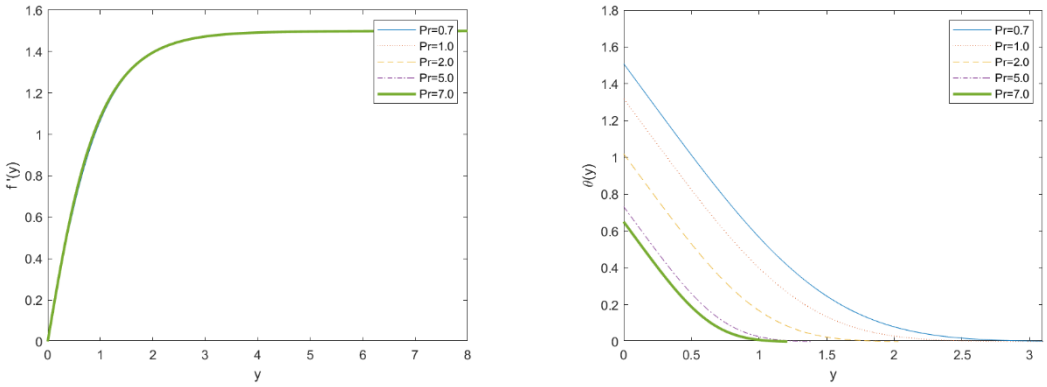

Figure 3 Velocity and Temperature profiles for different value of Pr.

In figure 3, velocity and temperature profiles of a hybrid nanofluid at $x \approx 0$ are shown, with varied Pr values for $K = 1, \emptyset = 0.1$, and $\lambda = 1$. Increasing Pr results in lower profiles, as viscous forces strengthen while thermal forces weaken. Velocity profiles remain similar across Pr values, indicating little influence. Higher Pr values lead to lower maximum temperatures at $y = 0$, with sharper profiles, while lower Pr values result in higher temperatures and more gradual drops. This highlights the significant impact of Prandtl number variations on temperature profiles and less influence on velocity profiles within the boundary layer.

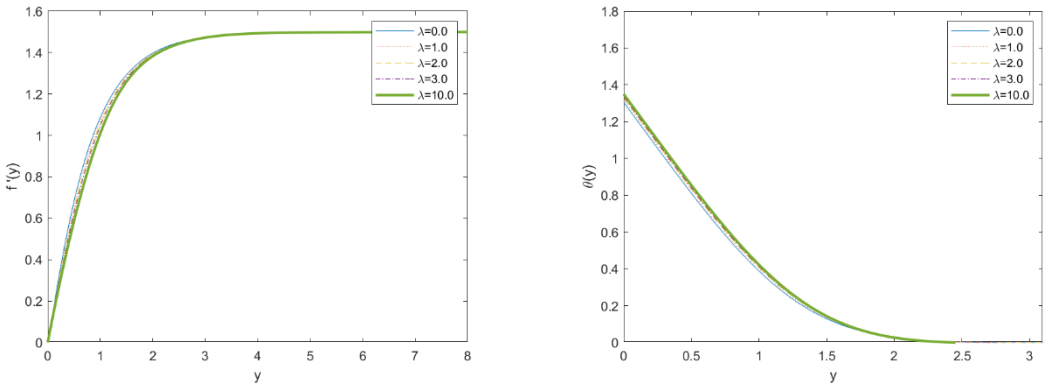

Figure 4 Velocity and Temperature profiles for different value of λ.

In figure 4, velocity and temperature profiles at $x \approx 0$ are depicted for varied λ values, with $K = 1, \emptyset = 0.1$, and $\mathrm{Pr} = 1$. Increasing λ reduces velocity profiles but elevates temperature profiles. As λ rises, velocity profiles steepen at the boundary and approach the asymptotic value faster. Curves converge to a steady-state value further from the boundary, indicating λ predominant influence near the border. Higher λ values yield higher initial temperatures near the border, decreasing sharply with increasing y. Conversely, lower λ values result in lower initial temperatures and a more gradual decline in the profile.

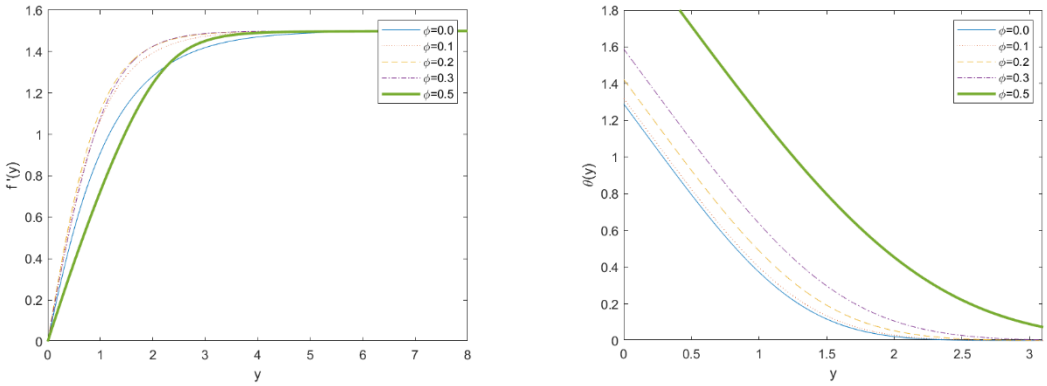

Figure 5 Velocity and Temperature profiles for different value of Ø.

In figure 5, velocity and temperature profiles at $x \approx 0$ are illustrated for varying ∅ values, with $K = 1, \lambda = 1$, and $\mathrm{Pr} = 1$. Increasing ∅ reduces velocity profiles and increases temperature profiles. Velocity rises from zero and approaches a constant value with increasing *y*, typical of boundary layer flows. Higher ∅ values yield more curved profiles near the origin, indicating a steeper gradient near the border. Temperature decreases with distance from the barrier, eventually reaching ambient temperature. Lower ∅ values result in a sharper temperature decline with *y*, while higher ∅ values lead to a more gradual temperature decrease with *y*. Therefore, considering *K, Pr,* λ, and ∅ values, the findings reveal that the mixed convection boundary layer flow of viscoelastic hybrid nanofluid with constant heat flux and thermal conductivity yields higher values in velocity profiles. When the velocity is higher, the heat transfer rate increases. It demonstrates how fluid motion may aid with heat transmission. As a result, temperature profiles show lower values.

Conclusion

The study investigates mixed convection flow of a hybrid nanofluid past a sphere with constant heat flux. Copper (Cu) and Aluminium Oxide ($\mathrm{Al_2O_3}$) nanoparticles are used with water ($\mathrm{H_2O}$) as base fluid. Results obtained through MATLAB's BVP4C solver reveal trends for varying viscoelastic parameter (*K*), Prandtl number (Pr), mixed convection parameter (λ), and nanoparticle volume percentage (∅). Increasing K, λ, and ∅ decreases velocity profiles but raises temperature profiles. Inversely, higher Pr decreases velocity and temperature profiles. Hybrid nanofluids exhibit enhanced heat transmission due to higher thermal conductivity, making them valuable in solar energy, medical, and electronics cooling applications.

References

[1] Ahmed, M. S., Hady, M. R. A., & Abdallah, G. (2018). Experimental investigation on the performance of chilled-water air conditioning unit using alumina nanofluids. *Thermal Science and Engineering Progress*, *5*, 589-596. https://doi.org/10.1016/j.tsep.2017.07.002

[2] Ahmed, M. S., & Elsaid, A. M. (2019). Effect of hybrid and single nanofluids on the performance characteristics of chilled water air conditioning system. *Applied Thermal Engineering*, *163*, 114398. https://doi.org/10.1016/j.applthermaleng.2019.114398

[3] Akbar, Y., Abbasi, F. M., & Shehzad, S. A. (2020). Effectiveness of Hall current and ion slip on hydromagnetic biologically inspired flow of Cu− Fe 3 O 4/H 2 O hybrid nanomaterial. *Physica Scripta*, *96*(2), 025210. https://dx.doi.org/10.1088/1402-4896/abcff1

[4] Rivlin, R. S. "Large elastic deformations of isotropic materials IV. Further developments of the general theory." *Philosophical Transactions of the Royal Society of London. Series A, Mathematical and Physical Sciences* 241, no. 835 (1948): 379-397. https://doi.org/10.1098/rsta.1948.0024

[5] Min, B. K., H. Kolsky, and A. C. Pipkin. "Viscoelastic response to small deformations superposed on a large stretch." *International Journal of Solids and Structures* 13, no. 8 (1977): 771-781. https://doi.org/10.1016/0020-7683(77)90112-3

[6] Bird, R. Byron. "Slow viscoelastic radial flow between parallel disks." *Applied Scientific Research* 33, no. 5-6 (1977): 385-404. https://doi.org/10.1007/BF00411821

[7] Harnoy, A. "An investigation into the flow of elastico-viscous fluids past a circular cylinder." *Rheologica Acta* 26, no. 6 (1987): 493-498. https://doi.org/10.1007/BF01333732

[8] Kasim, Abdul Rahman Muhd. "Convective boundary layer flow of viscoelastic fluid." *PhD. Thesis, Universiti Teknologi Malaysia, Faculty of Science* (2014).

[9] Jackson, J. D., Cotton, M. A., & Axcell, B. P. (1989). Studies of mixed convection in vertical tubes. *International journal of heat and fluid flow*, *10*(1), 2-15. https://doi.org/10.1016/0142-727X(89)90049-0

[10] Waini, I., Ishak, A., Groşan, T., & Pop, I. (2020). Mixed convection of a hybrid nanofluid flow along a vertical surface embedded in a porous medium. *International Communications in Heat and Mass Transfer*, *114*, 104565. https://doi.org/10.1016/j.icheatmasstransfer.2020.104565

[11] Al-Farhany, K., & Abdulsahib, A. D. (2021). Study of mixed convection in two layers of saturated porous medium and nanofluid with rotating circular cylinder. *Progress in Nuclear Energy*, *135*, 103723. https://doi.org/10.1016/j.pnucene.2021.103723

[12] Haq, I., Bilal, M., Ahammad, N. A., Ghoneim, M. E., Ali, A., & Weera, W. (2022). Mixed convection nanofluid flow with heat source and chemical reaction over an inclined irregular surface. *ACS omega*, *7*(34), 30477-30485. https://doi.org/10.1021/acsomega.2c03919

[13] Cimpean, D. S., Sheremet, M. A., & Pop, I. (2020). Mixed convection of hybrid nanofluid in a porous trapezoidal chamber. *International Communications in Heat and Mass Transfer*, *116*, 104627. https://doi.org/10.1016/j.icheatmasstransfer.2020.104627

[14] Mahat, R., Shafie, S., & Januddi, F. (2021). Numerical analysis of mixed convection flow past a symmetric cylinder with viscous dissipation in viscoelastic nanofluid. *CFD letters*, *13*(2), 12-28. https://doi.org/10.37934/cfdl.13.2.1228

[15] Mahat, R., Saqib, M., Ulah, I., Shafie, S., & Isa, S. M. (2022). Magnetohydrodynamics Mixed Convection of Viscoelastic Nanofluid Past a Circular Cylinder with Constant Heat Flux. *CFD Letters*, *14*(9), 52-59. https://doi.org/10.37934/cfdl.14.9.5259

[16] Gamachu, D., & Ibrahim, W. (2021). Mixed convection flow of viscoelastic Ag-Al2O3/water hybrid nanofluid past a rotating disk. *Physica Scripta*, *96*(12), 125205. https://dx.doi.org/10.1088/1402-4896/ac1a89

[17] Ibrahim, W., & Gamachu, D. (2022). Entropy generation in radiative magneto-hydrodynamic mixed convective flow of viscoelastic hybrid nanofluid over a spinning disk. *Heliyon*, *8*(12). https://doi.org/10.1016/j.heliyon.2022.e11854

[18] Devi, S. A., & Devi, S. S. U. (2016). Numerical investigation of hydromagnetic hybrid Cu–Al2O3/water nanofluid flow over a permeable stretching sheet with suction. *International Journal of Nonlinear Sciences and Numerical Simulation*, *17*(5), 249-257. https://doi.org/10.1515/ijnsns-2016-0037

[19] Ali, B., Mishra, N. K., Rafique, K., Jubair, S., Mahmood, Z., & Eldin, S. M. (2023). Mixed convective flow of hybrid nanofluid over a heated stretching disk with zero-mass flux using the modified Buongiorno model. *Alexandria Engineering Journal*, *72*, 83-96. https://doi.org/10.1016/j.aej.2023.03.078

[20] Alzu'bi, O. A. S., Alwawi, F. A., Swalmeh, M. Z., Sulaiman, I. M., Hamarsheh, A. S., and Ibrahim, M. A. H. (2022). Energy Transfer through a Magnetized Williamson Hybrid Nanofluid Flowing around a Spherical Surface: Numerical Simulation. *Mathematics*, *10*(20). https://doi.org/10.3390/math10203823

[21] Salleh, S. N. A., Bachok, N., and Pop, I. (2021). Mixed convection stagnation point flow of a hybrid nanofluid past a permeable flat plate with radiation effect. *Mathematics*, *9*(21), 3323–3333. https://doi.org/10.3390/math9212681

[22] Merkin, J. H. (1994). Natural-convection boundary-layer flow on a vertical surface with Newtonian heating. *International Journal of Heat and Fluid Flow*, *15*(5), 392–398. https://doi.org/10.1016/0142-727X(94)90053-1

[23] Patil, P. M., Shankar, H. F., Hiremath, P. S., & Momoniat, E. (2021). Nonlinear mixed convective nanofluid flow about a rough sphere with the diffusion of liquid hydrogen. *Alexandria Engineering Journal*, *60*(1), 1043–1053. https://doi.org/10.1016/j.aej.2020.10.029

[24] Kamil, A. A. M. (2022). Solving Thermal Radiation on Boundary Layer Flow Using BVP4 C Technique. Enhanced Knowledge in Sciences and Technology, 2(1), 048-055. https://doi.org/10.30880/ekst.2022.02.01.006

[25] Sohut, F. H., Soid, S. K., & Ishak, A. (2023). A GUI for computing hybrid nanofluid boundary layer flow using bvp4c Solver in MATLAB: educational purposes for university students. Journal of Advanced Research Design, 103(1), 1-11. https://doi.org/10.37934/ard.103.1.111